

論文 / 著書情報
Article / Book Information

Title	Tellurite Glass Micro-Superspheres as Broadband Raman Resonator
Authors	Yusuke Arai, Guanshi Qin, Takenobu Suzuki, Yasutake Ohishi, Tetsuji Yano, Shuichi Shibata
Citation(English)	SPIE Photonics West 2008, Vol. 6890, No. , pp. 6890-09
発行日 / Pub. date	2008, 1
DOI	http://dx.doi.org/10.1117/12.763030
権利情報 / Copyright	<p>本著作物の著作権はSociety of Photo-Optical Instrumentation Engineersに帰属します。 Copyright 2008 Society of Photo-Optical Instrumentation Engineers. One print or electronic copy may be made for personal use only. Systematic reproduction and distribution, duplication of any material in this paper for a fee or for commercial purposes, or modification of the content of the paper are prohibited.</p>

Tellurite glass micro-superspheres as broadband Raman resonator

Yusuke Arai, Guanshi Qin, Takenobu Suzuki and Yasutake Ohishi^a,
Tetsuji Yano and Shuichi Shibata^b

^aResearch Center for Advanced Photon Technology, Toyota Technological Institute,
2-12-1 Hisakata Tempaku-ku, Nagoya 468-8511, Japan;

^bTokyo Institute of Technology, 2-12-1 Ookayama Meguro-ku, Tokyo 152-8550, Japan.

ABSTRACT

Tellurite glass micro-superspheres (Te- μ SSs) were prepared by the surface-tension mold (StM) technique, and their whispering gallery mode (WGM) resonances have been investigated as the first trial to realize an ultra-broadband Raman resonator. Micrometer-sized tellurite glass particles were melted on an optical grade glassy-carbon substrate then cooled to room temperature (StM technique). Resultant Te- μ SS possesses a super-spherical shape with high optical transparency. The size of the partly truncated area, resulting from the contact surface with the substrate, can be controlled by the composition of the glass and a microsphere with no truncated area was achieved for a glass with 56TeO₂-3.5BaO-10.5SrO-8Nb₂O₅-4WO₃-16P₂O₅ (TBSN-4W-16P) composition. The TBSN-4W-16P μ SS was excited at 532 nm, and the WGM resonance emission attributed to broad Raman scattering of the glass itself was observed. The Q value of the μ SS was $\approx 5 \times 10^3$. It was confirmed that the prepared μ SSs possess a sufficiently spherical shape and acted as an efficient WGM resonator. These results predict that the Te- μ SS has potential for a novel broadband Raman laser.

Keywords: tellurite glass, whispering gallery mode resonance, broadband Raman resonator, surface tension mold technique

1. INTRODUCTION

Broadband amplifiers in near-infrared region are key devices for the future photonic network systems. Many attempts have been made on broadening and flattening of gain spectra of erbium ion-doped fiber amplifiers (EDFA).¹⁻³ In addition, much work has been done to expand the usable bandwidth for wavelength division multiplexing (WDM) systems; connecting the several rare-earth-doped fiber amplifiers (RDFA), containing different rare earth ions, in series or in parallel, for instance. Fluoride and heavy metal oxide glasses have been studied as host materials for RDFAs to expand these amplification bandwidth because these glasses have low energy phonons compared with SiO₂ glasses and many rare earth ions are optically active in them.¹ This approach has contributed much to expand the gain bandwidth of rare earth ions, however, there is still a need to explore the materials themselves that have good thermal stability and optical performances. Additionally, the gain bandwidth of each rare-earth ion is limited due to narrow nature of $f - f$ transitions, hence the gain band of several connected RDFAs is still discontinuous. Fiber Raman amplifiers (FRA) have been gathering much attention because the gain bandwidth of FRA is only restricted by the pump wavelength and Raman active modes of the medium itself.⁴ The silica and germanium-doped silica glasses are currently used as Raman gain media in telecommunications industry. However, the FRA based on these glasses have very low Raman gain response and limited usable spectral bandwidth of around 5 THz for single pump excitation. Therefore, research for new materials with enhanced Raman gain coefficients and/or bandwidths has been undertaken by many researchers.⁵⁻⁹

Tellurite glasses are a promising candidate for FRAs and lasers¹⁰ because they have ~ 30 times higher Raman gain coefficients and much larger Stokes shift than silica glass.^{5,6} It has added advantages, such as: wide transmission window,¹¹ good glass stability and durability,¹⁰ high refractive index,¹² higher nonlinear optical properties¹³ and relatively low phonon energies.

Recently, we reported a new TeO₂-BaO-SrO-Nb₂O₅ (TBSN) tellurite glass system to enhance the gain bandwidth of tellurite glasses.^{7,14-17} The gain bandwidth of TBSN glasses were wider than that of the conventional tellurite glasses,¹⁴ and the bandwidth was spread by the addition of WO₃ and P₂O₅ while maintaining higher gain coefficients.^{16,17}

Further author information: E-mail: yusukea@toyota-ti.ac.jp, Telephone: +81 52 809 1862, Fax: +81 52 809 1869

On the other hand, novel micro-optical cavities are also desirable to realize the all-optical integrated circuit. Of growing interest among such micro-optical cavities is a whispering-gallery mode (WGM) resonators in a microsphere because of its high quality factor (Q).¹⁸ There have several reports of WGMs in microspheres, and various techniques of preparing microspheres has been developed: melting a tip of a SiO₂ fiber with a CO₂ laser,¹⁸ microwave plasma torch,¹⁹ liquid-liquid phase separation of BaO-B₂O₃ glass,²⁰ vibrating orifice technique^{21,22} and so on.

In our previous work, the novel preparation method of micrometer-sized superspheres (μ SS) named Surface-tension Mold (StM) technique has been developed.²³⁻²⁷ This technique uses the self-organization of glass melts driven by the surface tension of the droplet on the substrate, and μ SSs with very smooth spherical surface can be prepared easily. We have confirmed the WGMs from Eu₂O₃-doped Na₂O-CaO-SiO₂ μ SSs with a estimated $Q \geq 10^3$, under the 514.5 nm laser excitation.²³ We have also confirmed the partly truncated area of the μ SS which results from contact between the surface and the substrate, can be readily controlled by the composition of the glass.²⁷

The Q values of WGM resonances depend on sphericity, surface condition, diameter and refractive index of the microsphere.²⁸ The presence of truncated area suppress the Q of the μ SS. The glasses with lower wettability, i.e. higher surface tension (surface energy), are preferable, because the size of the truncated area depends on the wettability of the glass against the substrate. Therefore, if the tellurite glass μ SS is realized, it is expected to be a high- Q micrometer-sized broadband Raman resonator, because tellurite glasses possess not only high Raman coefficients, but also high refractive indices and high surface energies.

In this report, preparation of tellurite glass μ SSs and investigation of their optical functionality as broadband Raman resonator are presented.

2. EXPERIMENTAL

2.1 Sample preparation

All glasses were prepared following a conventional melt-quenching technique using TeO₂ (99.9 %), BaCO₃ (99 %), SrCO₃ (99.9 %), Nb₂O₅ (99.9 %), WO₃ (99.9 %), and P₂O₅ (99 %). The prepared compositions are summarized in Table 1. Appropriate amounts of these chemicals were mixed in a zirconia mortar and pestle inside a glove box with a dry nitrogen atmosphere. The mixed powders (~ 10g) were melted in a platinum crucible at 900 - 1000 °C for ~ 20 min using an electrical furnace with a dry oxy-nitrogen atmosphere. The melt was then quenched onto a preheated copper plate to ~ 350°C and subsequently annealed at this temperature for ~ 10h to release the thermal stresses developed during quenching process. A part of the melt was quenched to room temperature and kept without annealing for thermal analysis.

The bulk glass samples were cut to a thickness of 1 - 2 mm and polished to optical quality before subjecting them to the optical measurements. A part of the obtained glass was crushed and classified by using sieves in order to obtain the glass particles with sizes from 32 - 63 μ m. Then the particles were dispersed on the finely polished glassy carbon (g-carbon) substrate. The particles on g-carbon substrate were heated up to a certain temperature ($T_s + 50 \sim 100^\circ\text{C}$ where T_s is softening temperature of the glass) and held for 30 min under the nitrogen atmosphere, and then cooled to the room temperature. The heating rate and cooling rate were 10 °C/min.

2.2 Characterization

Thermal properties of prepared glasses were studied by a differential scanning calorimeter (Rigaku, ThermoPlus DSC 8270). About 50 mg of the finely powdered as-quenched glasses were heated in a platinum pan at a rate of 10 °C/min in the 30 - 900 °C range. Glass transition temperatures (T_g), softening temperatures (T_s) and first crystallization temperatures (T_{x1}) of the glasses were obtained from DSC curves. The T_g and T_{x1} were determined from the tangent intersections of the endothermic peak and the first exothermic peak in the DSC curves, respectively. The T_s were obtained from the peak temperatures of the first endothermic peak.

The obtained glass particles were observed by the scanning electron microscope (SEM) and optical microscope (OM) to obtain the particle shape (the sphericity and the contact angle of the truncated part), surface roughness, and the optical transparency. Figure 1 shows the schematic illustration of the glass droplet on a g-carbon substrate. The contact angle θ was calculated from the SEM images using the equation as follows:

$$\theta = \arcsin\left(\frac{r}{R}\right), \quad (1)$$

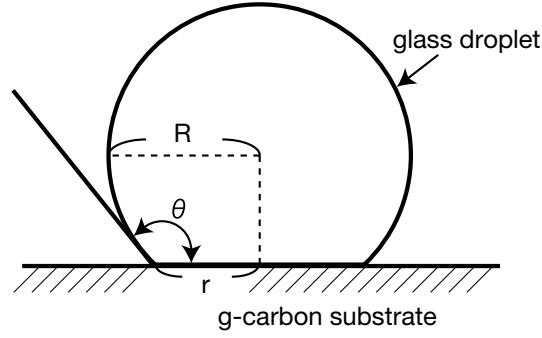


Figure 1. Schematic illustration of the glass droplet on a g-carbon substrate.

where r is a radius of the truncated area and R is a radius of the particle.

The ordinary Raman spectra of the glasses were measured by a Raman spectrometer (JASCO, NRS 2100) in the 25 to 1700 cm^{-1} range. The samples were excited at 532 nm with power of 5 ~ 100 mW. The spectrum was recorded in the quasi-back scattered mode with v/v polarization. The measured Raman intensities were corrected using the following equation:

$$I_{corr} = \frac{\nu}{(\nu_0 - \nu)^4} \left[1 - \exp\left(-\frac{h\nu}{kT}\right) \right] \times I_{obs}, \quad (2)$$

where I_{corr} is the corrected intensity, I_{obs} is the measured intensity, ν_0 is the frequency of the excitation light, ν is the Raman shift, h is the Planck's constant, and T is the absolute temperature.

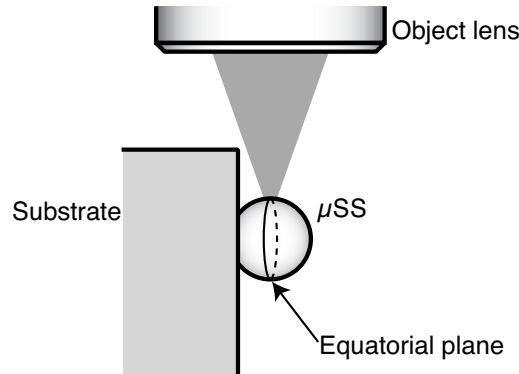


Figure 2. Schematic illustration of the setup of the μSS for emission spectra measurements.

The WGM resonance spectra of the μSS s were measured by a microscopic Raman spectrometer (JASCO, NRS 2100) in the 25 - 1700 cm^{-1} range. The μSS attached on the substrate was placed on the precision optic liner stage (Newport, ULTRAlign 561D-XYZ). The substrate was set vertically as shown in Fig. 2. The μSS was excited at 532 nm with a power of 5 ~ 100 mW. The spectrum was recorded in the microscopic co-focal mode with v/v polarization. The spectral resolution of the monochromator was 1 cm^{-1} . The sizes of the examined μSS s were measured from the captured images by CCD camera equipped in Raman microscope.

3. RESULTS AND DISCUSSION

The glass transition temperature (T_g), softening temperature (T_s) and the first crystallization temperature (T_{x1}) of prepared glasses are summarized in Table 1. The T_g , T_s and T_{x1} of TBSN glasses was confirmed to increase due to WO_3 and P_2O_5 doping. $\Delta T = T_{x1} - T_g$, this indicates the thermal stability of the glass and is also shown in the Table 1. During the StM process the glass powders are heated up to $T_s + 50 \sim 100^\circ\text{C}$, thus higher thermal stability is desirable. ΔT increased with increasing WO_3 and P_2O_5 contents, and the highest $\Delta T = 238$ was achieved in TBSN-4W-16P composition.

Table 1. Compositions and thermal properties of the glass samples. T_g , T_s and T_{x1} are glass transition temperature, softening temperature and first crystallization temperature of the glass, respectively. $\Delta T = T_{x1} - T_g$ is the thermal stability of the glass.

Name	Glass composition	T_g ($^\circ\text{C}$)	T_s ($^\circ\text{C}$)	T_{x1} ($^\circ\text{C}$)	ΔT
TBSN	78TeO ₂ -3.5BaO-10.5SrO-8Nb ₂ O ₅	387	412	471	84
TBSN-4W-0P	74TeO ₂ -3.5BaO-10.5SrO-8Nb ₂ O ₅ -4WO ₃	395	427	497	102
TBSN-8W-0P	70TeO ₂ -3.5BaO-10.5SrO-8Nb ₂ O ₅ -8WO ₃	404	441	538	134
TBSN-4W-8P	66TeO ₂ -3.5BaO-10.5SrO-8Nb ₂ O ₅ -4WO ₃ -8P ₂ O ₅	410	437	602	192
TBSN-0W-16P	62TeO ₂ -3.5BaO-10.5SrO-8Nb ₂ O ₅ -16P ₂ O ₅	429	468	642	213
TBSN-2W-16P	60TeO ₂ -3.5BaO-10.5SrO-8Nb ₂ O ₅ -2WO ₃ -16P ₂ O ₅	431	471	668	237
TBSN-4W-16P	56TeO ₂ -3.5BaO-10.5SrO-8Nb ₂ O ₅ -4WO ₃ -16P ₂ O ₅	437	476	675	238

Figure 3 shows the SEM images of the bottom-side of the obtained glass particles with the diameter of about 35 μm . All of the glass particles formed superspherical shape as shown in Fig. 3 except for the TBSN-4W-0P composition. Bubbles were observed at the truncated area, which was the contact surface with the g-carbon substrate. The largest bubbles were confirmed in TBSN-4W-0P. The bubbles were not observed at the top-side of the particles, thus these were caused by the reaction between the g-carbon substrate and some gases, which was most likely O_2 eliminated from the TBSN glasses. This reactivity decreased with increasing WO_3 and P_2O_5 contents, hence the surface defects were almost eliminated in TBSN- x W-16P μSSs .

Figure 4 shows the dependence of the contact angle θ on the (a) P_2O_5 and (b) WO_3 contents. θ varies linearly with both of P_2O_5 and WO_3 contents. At high temperatures glass becomes a viscous 'liquid' and has a high surface tension. On a g-carbon substrate, the forces of the surface tension are balanced according to Young-Dupre's equation:^{29,30}

$$\cos \theta = \frac{\gamma_s - \gamma_{SL}}{\gamma_L}, \quad (3)$$

where γ_s , γ_L , and γ_{SL} are the surface tension of the substrate, liquid, and the interface tension between the liquid and the substrate, respectively. From Eq. (3), larger surface tension of the glass melt increases the contact angle θ . The results shown in Fig. 4 suggest that the surface tension of the TBSN system is increased by addition of P_2O_5 and WO_3 .

Figure 5 shows (a) OM and (b) SEM images of the TBSN-4W-16P glass particle. Figure 5 (a) is the side-view, and Fig. 5 (b) is the top-view of the particle. All of the TBSN-4W-16P glass particles possess a smooth surface, high sphericity with large contact angle, and optical transparency. High sphericity of the particle surface shown in Fig. 5 (a) reveals that the effect of gravity to asphericity is small, and the surface tension of the melt determines the shape of the particle in the micrometer-size region. Figure 6 shows the plot of the contact angle θ against the diameter of the μSSs . θ increased with decreasing the diameter, and $\theta = 180^\circ$, i.e. microsphere with no truncated area, was achieved when the diameter was smaller than 40 μm .

Figure 7 (a) shows a Raman spectrum of TBSN-4W-16P glass. The spectrum was corrected for intensity by Eq. (2). The broad Raman band, centered at 780 cm^{-1} with 360 cm^{-1} full-width-half-maximum (FWHM), was observed. Figure 7 (b) shows the Raman spectrum of a TBSN-4W-16P μSS with a diameter of 37 μm . Periodic sharp peaks attributed to WGM resonances are observed. These peaks were observed even when pumped at the lowest power of 5 mW, and increased in intensity with increasing pumping power.

According to the Lorenz-Mie theory, a mode spacing $\Delta\nu$ is known to correlate with the diameter of the microsphere d and refractive index n as follows:²⁸

$$\Delta\nu \approx \frac{1}{\pi d} \cdot \frac{\tan^{-1}(n^2 - 1)^{1/2}}{(n^2 - 1)^{1/2}}. \quad (4)$$

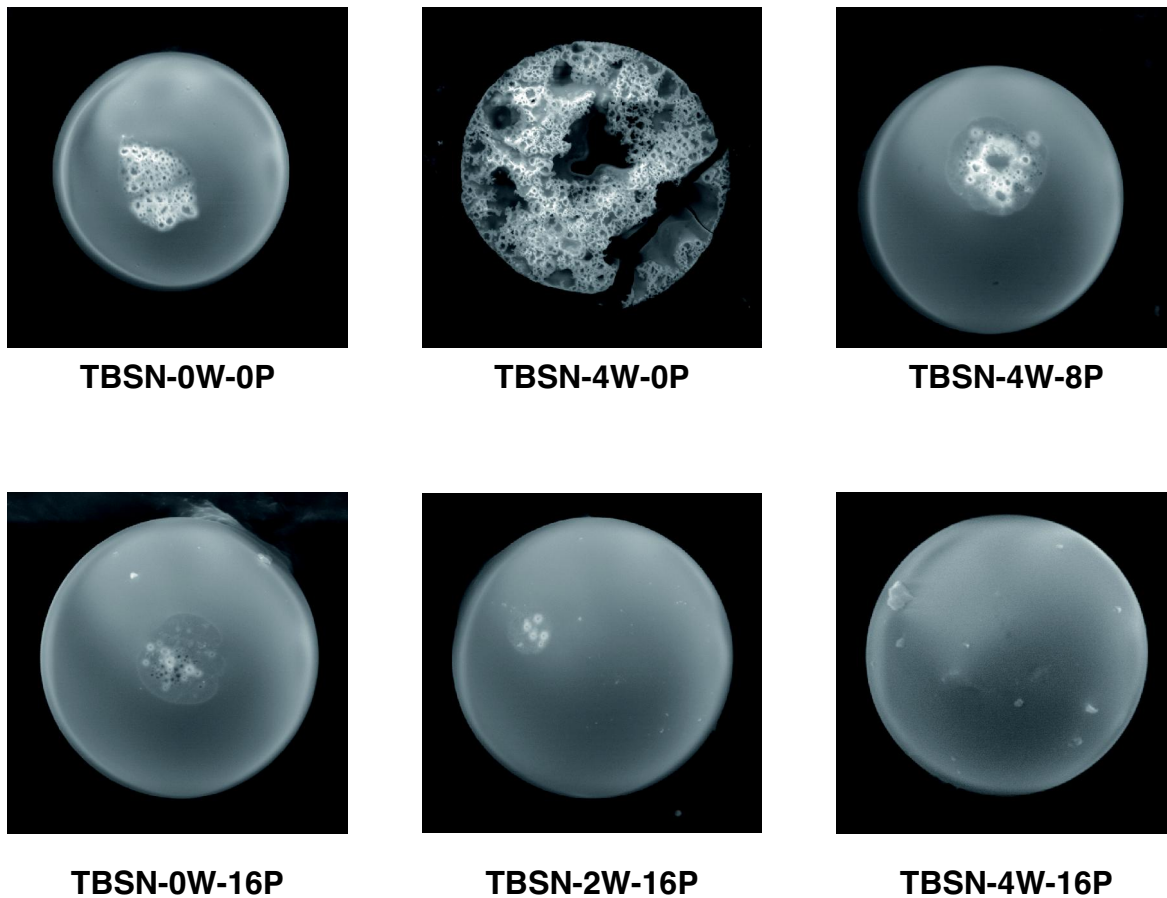


Figure 3. SEM images of the bottom-side of the obtained glass particles with the diameter of about 35 μm .

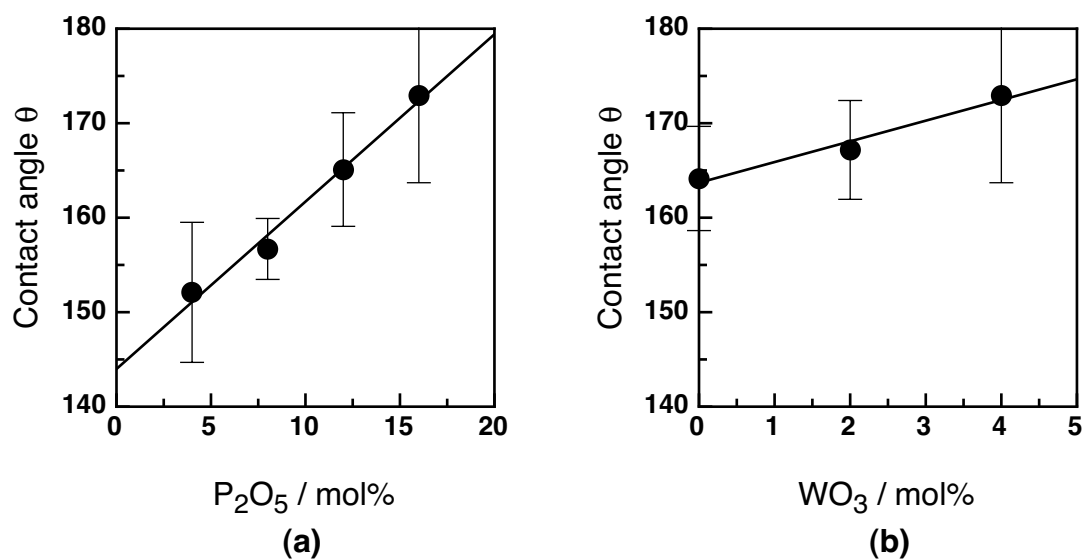


Figure 4. Variation of the contact-angle θ against the (a) P_2O_5 and (b) WO_3 contents. The compositions of the samples are (a) TBSN-4W- x P ($x = 0 \sim 16$) and (b) TBSN- x W-16P ($x = 0 \sim 4$), respectively.

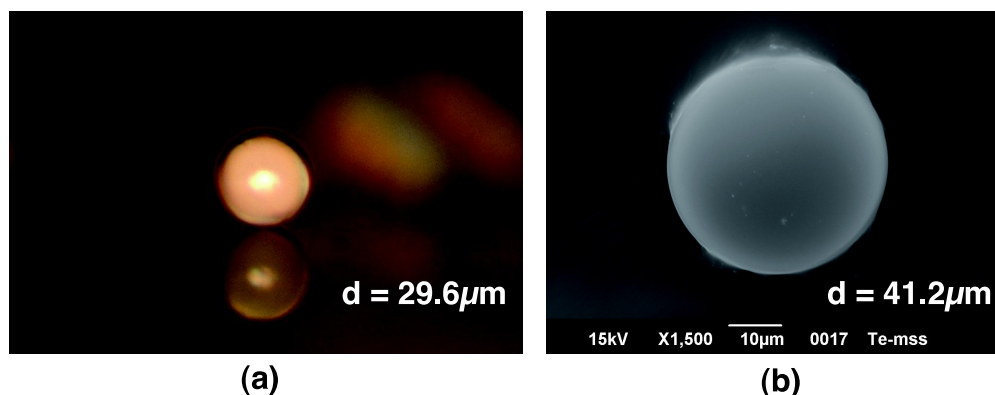


Figure 5. (a) Optical microscope and (b) SEM images of TBSN-4W-16P μ SSs. (a) is the side-view, and (b) is the top-view of the μ SS.

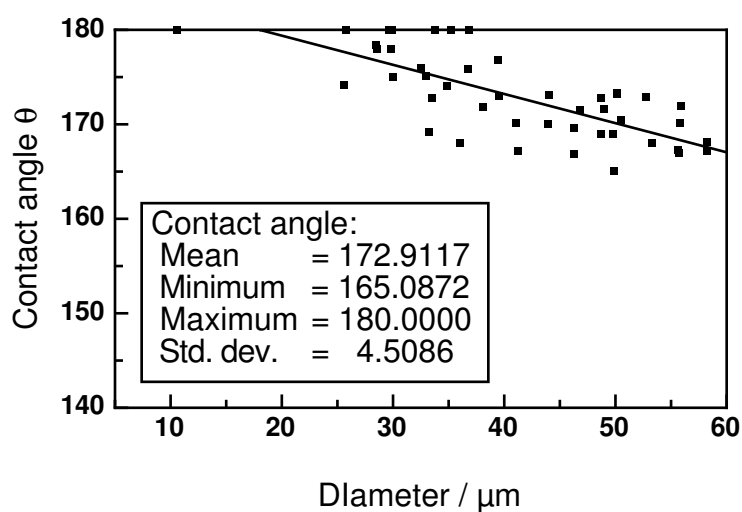


Figure 6. Contact angle θ against the diameter of the TBSN-4W-16P μ SSs.

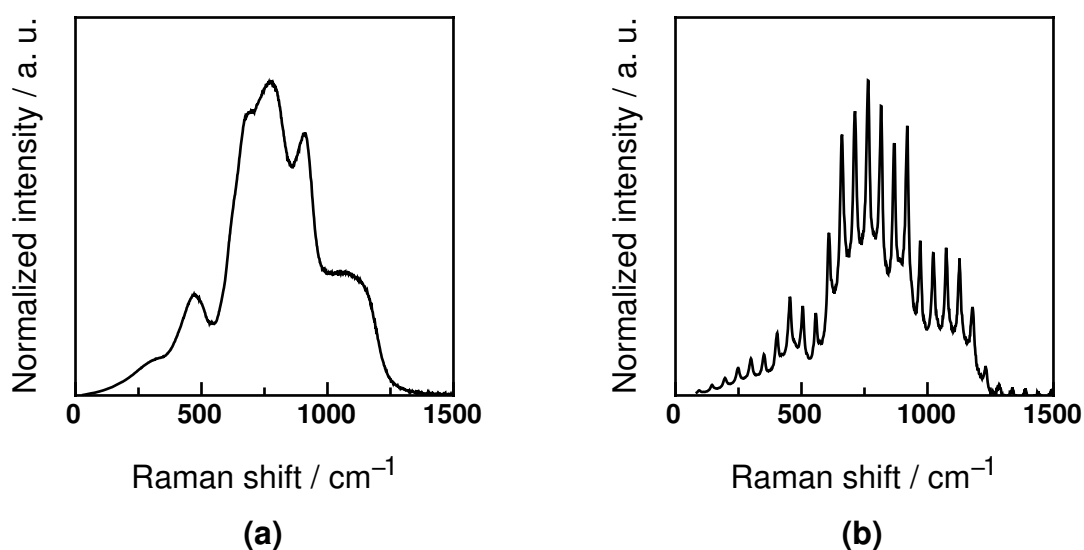


Figure 7. (a) Raman scattering spectra of the TBSN-4W-16P bulk glass and (b) WGM resonance spectrum of the TBSN-4W-16P μ SS.

The calculated $\Delta\nu$ using the values of $n = 1.98$ and $d = 37\mu\text{m}$ is 51cm^{-1} , and it corresponds well with measured $\Delta\nu = 52\text{cm}^{-1}$. The Q values of these peaks were estimated from the equation, $Q = \omega_0/\Delta\omega$, where ω_0 and $\Delta\omega$ is the center frequency and the FWHM of the resonance peak, respectively. From the spectrum in Fig. 7 (b), Q was calculated to 5×10^3 . Therefore, the prepared TBSN-4W-16P μSSs were considered to have the sufficiently spherical shape and act as an efficient WGM resonator.

4. SUMMARY

Tellurite glass micro-superspheres (Te- μSSs) were prepared by the StM technique, and their WGM resonances have been investigated as the first trial to realize an ultra-broadband Raman resonator. Micrometer-sized tellurite glass particles were melted on a glassy-carbon substrate with a surface of optical grade and cooled to room temperature. Resultant Te- μSS possesses a super-spherical shape with high optical transparency. The size of the partly truncated area, resulting from the contact between the surface and the substrate, can be controlled by the composition of the glass, and a microsphere with no truncated area was achieved for a glass with $56\text{TeO}_2\text{-}3.5\text{BaO-}10.5\text{SrO-}8\text{Nb}_2\text{O}_5\text{-}4\text{WO}_3\text{-}16\text{P}_2\text{O}_5$ (TBSN-4W-16P) composition. The TBSN-4W-16P μSS was excited at 532 nm, and the WGM resonance emission attributed to broad Raman scattering of the glass itself was observed. The Q value of the μSS was $\approx 5 \times 10^3$ and the prepared μSSs possess the sufficiently spherical shape and also acted as an efficient WGM resonator. These results predict that the Te- μSS has a potential for the novel broadband Raman lasers.

4.1 Acknowledgments

This work was supported in part by MEXT, the Private University High-Tech Research Center Program (2006-2010).

REFERENCES

1. W. J. Miniscalco, "Erbium-doped glasses for fiber amplifiers at 1500 nm," *IEEE J. Lightwave Technol.* **9**, p. 234-250, 1991.
2. M. Semenkoff, M. Guibert, D. Ronarc'h, Y. Sorel, and J. F. Kerdiles, "Improvement of gain flatness of optical fluoride fiber amplifiers for multiwavelength transmission," *J. Non-Cryst. Solids* **184**, pp. 240-243, 1995.
3. Y. Ohishi, "Ultrabroadband optical amplifiers for WDM," in *Proc. of SPIE* **5246**, pp. 163-173, 2003.
4. M. N. Islam, *Raman Amplification for Telecommunications*, ch. 1, pp. 1-34. Springer-Verlag, New York, 2004.
5. A. Mori, H. Masuda, K. Shikano, and M. Shimizu, "Ultra-wide-band tellurite-based fiber Raman amplifier," *J. Lightwave Technol.* **21**, pp. 1300-1306, 2003.
6. R. Stegeman, L. Jankovic, H. Kim, C. Rivero, G. Stegeman, K. Richardson, P. Delfyett, Y. Guo, A. Schulte, and T. Cardinal, "Tellurite glasses with peak absolute Raman gain coefficients up to 30 times that of fused silica," *Opt. Lett.* **28**, pp. 1126-1128, 2003.
7. G. S. Murugan, T. Suzuki, and Y. Ohishi, "Tellurite glasses for ultrabroadband fiber Raman amplifiers," *Appl. Phys. Lett.* **86**, pp. 161109-1-161109-3, 2005.
8. V. G. Plotnichenko, V. O. Sokolov, V. V. Koltashev, E. M. Dianov, I. A. Grishin, and M. F. Churbanov, "Raman band intensities of tellurite glasses," *Opt. Lett.* **30**, pp. 1156-1158, 2005.
9. R. Stegeman, C. Rivero, K. Richardson, G. Stegeman, J. Peter Delfyett, Y. Guo, A. Pope, A. Schulte, T. Cardinal, P. Thomas, and J.-C. Champarnaud-Mesjard, "Raman gain measurements of thallium-tellurium oxide glasses," *Opt. Express* **13**, pp. 1144-1149, 2005.
10. J. S. Wang, E. M. Vogel, and E. Snitzer, "Tellurite glass: a new candidate for fiber devices," *Opt. Mater.* **3**, pp. 187-203, 1994.
11. D. R. Ulrich, "Electrical and optical properties of glasses in bismuth trioxide-tellurium dioxide system," *J. Am. Ceram. Soc.* **47**, pp. 595-596, 1964.
12. H. Bürger, K. Kneipp, H. Hobert, W. Vogel, V. Kozhukharov, and S. Neov, "Glass formation, properties and structure of glasses in the $\text{TeO}_2\text{-ZnO}$ system," *J. Non-Cryst. Solids* **151**, pp. 134-142, 1992.
13. G. S. Murugan, T. Suzuki, Y. Ohishi, Y. Takahashi, Y. Benino, T. Fujiwara, and T. Komatsu, "Second harmonic generation in transparent surface crystallized glasses in the $\text{BaO-B}_2\text{O}_3\text{-TeO}_2$ system," *Appl. Phys. Lett.* **85**, pp. 3405-3407, 2004.

14. G. S. Murugan and Y. Ohishi, "TeO₂-BaO-SrO-Nb₂O₅ glasses: A new glass system for waveguide devices applications," *J. Non-Cryst. Solids* **341**, pp. 86–92, 2004.
15. G. S. Murugan and Y. Ohishi, "Raman spectroscopic studies of TeO₂-BaO-SrO-Nb₂O₅ glasses: Structure - property correlations," *J. Appl. Phys.* **96**, pp. 2437–2442, 2004.
16. R. Jose and Y. Ohishi, "Enhanced Raman gain coefficients and bandwidths in P₂O₅ and WO₃ added tellurite glasses for Raman gain media," *Appl. Phys. Lett.* **89**, pp. 121122–1 – 121122–3, 2006.
17. Y. Ohishi and R. Jose, "Raman scattering characteristics of WO₃ and P₂O₅ doped TBSN glasses: a new gain medium for broadband fiber Raman amplifiers (invited paper)," in *Proc. of SPIE* **6389**, pp. 638906–1 – 638906–13, 2006.
18. S. M. Spillane, T. J. Kippenberg, and K. J. Vahala, "Ultralow-threshold Raman laser using a spherical dielectric microcavity," *Nature* **415**, pp. 621–623, 2002.
19. F. Lissillour, P. Féron, N. Dubreuil, P. Dupriez, and G. M. Stéphan, "Whispering-gallery mode Er-ZBLAN microlasers at 1.56 μ m," in *Proc. of SPIE* **3611**, pp. 199–205, 1999.
20. T. Konishi, K. Soga, H. Inoue, and A. Makishima, "Synthesis and properties of glassy microcavities for morphology-dependent resonances through liquid-liquid phase separation," *J. Am. Ceram. Soc.* **85**, pp. 1151–1156, 5 2002.
21. S. Shibata, A. Tomizawa, H. Yoshikawa, T. Yano, and M. Yamane, "Preparation of spherical particles by vibrating orifice technique," in *Proc. of SPIE* **3943**, pp. 112–119, 2000.
22. Y. Arai, T. Yano, and S. Shibata, "High refractive-index microspheres as optical cavity structure," *J. of Sol-Gel Sci. and Tech.* **32**, pp. 189–194, 2004.
23. T. Kishi, S. Shibata, and T. Yano, "Preparation of micrometer size super spherical glasses for optical resonator," in *Proc. of XX International Congress on Glass*, O–14–022, (Kyoto, Japan), 2004.
24. T. Kishi, S. Shibata, and T. Yano, "Fabrication of SIL array of glass by surface-tension mold technique," in *Proc. of SPIE* **6126**, pp. 61260P-1 – 61260P-8, 2006.
25. T. Yano, S. Shibata, and T. Kishi, "Fabrication of micrometer-size glass solid immersion lens," *Appl. Phys. B* **83**, pp. 167–170, 2006.
26. T. Kishi, S. Shibata and T. Yano, "Fabrication of high-refractive-index glass micron-sized solid immersion lenses by a surface-tension mold technique" *J. Non-Cryst. Solids*, 2007, doi:10.1016/j.jnoncrysol.2007.07.065.
27. T. Kishi, S. Shibata and T. Yano, "Fabrication of micrometer-size solid immersion lens: composition dependence of wettability of substrate by glass melt" *J. Non-Cryst. Solids*, 2007, doi:10.1016/j.jnoncrysol.2007.08.051
28. S. C. Hill, *Optical Effects Associated With Small Particles*, ch. 1, pp. 3–61. World Scientific, Singapore, 1988.
29. T. Young, "An essay on the cohesion of fluids," *Philos. Trans. Soc. London* **95**, p. 65, 1805.
30. A. Dupre, *Theorie Mecanique de la Chaleur*, p. 368. Gauthier-Villars, Paris, 1869.